

Redirecting the Coat Protein of a Spherical Virus to Assemble into Tubular Nanostructures

Santanu Mukherjee, Cory M. Pfeifer, Jennifer M. Johnson, Jay Liu, and Adam Zlotnick*

Department of Biochemistry and Molecular Biology, University of Oklahoma Health Sciences Center, 975 N.E. 10th Street, Oklahoma City, Oklahoma 73104

Received October 7, 2005; E-mail: adam-zlotnick@ouhsc.edu

Viral capsid proteins are building blocks that can be compelled to assemble into non-native configurations. These self-assembly properties can be exploited for the synthesis of nanostructures and as templates or scaffolding for more complex structures. Here we report a synthetic tubular nanostructure, not found in nature, prepared from the self-assembling capsid protein of a spherical virus.

The icosahedral capsid of cowpea chlorotic mottle virus (CCMV) is formed by 90 homodimers of 20 kDa coat protein (CP) arranged with $T = 3$ quasi-symmetry. The CP consists of 189 amino acids with an N-terminal RNA-binding domain that includes nine basic residues. Free CP is dimeric.¹ The structure of the virion is maintained by protein–RNA interactions and interdimer contacts that form turret-like capsomeres.² Capsid assembly in vitro is either induced by RNA at neutral pH or induced by low pH (~ 5) without RNA.¹ Although interactions between dimers are weak even at acidic pH, -3 kcal/mol, the network of interactions results in a globally stable structure;³ at neutral pH, empty capsids dissociate.¹ In vitro assembly at neutral pH is not specific for viral RNA and can be induced by other polyanions. Although the predominant form of assembled structure is spherical, other forms (multi-lamellar spheres and tubes) have also been observed.¹

Our goal in this study was to assemble a structure that can be used as a platform for building more complex nanostructures. Such structures have been the subject of recent investigations.^{4–9} To accomplish this goal, we focused on regulating CP assembly using different substrates. Here we examine assembly of CP on a DNA scaffold. We find that the geometry of CP controls the diameter of the resulting tubular structure. However, the length of the tubes is a distribution that reflects the assembly mechanism, with the longest tubes at an optimal ratio of CP and DNA.

We examined assembly of CP in the presence of a nonspecific 500-mer double-stranded DNA. We felt a uniform DNA was most likely to yield uniform products; in fact, other DNA—a 1000 base pair (bp) PCR-amplified product, a 7300 bp plasmid, or a 23 000 bp phage genome—yielded similar results (data not shown). After a 20 min incubation in 20 mM Tris-Cl, pH 7.5, 150 mM NaCl, assembly reactions were monitored by native gel electrophoresis in 0.6% agarose (Figure 1A). CP titrations of nonspecific DNA were reminiscent of similar experiments with RNA.¹⁰ At very low CP (0.01 μ M), DNA migration was unchanged, but the intensity of the ethidium bromide (ETBR) fluorescent stain was noticeably brighter. Increasing concentrations of CP slowed migration of DNA and caused the DNA band to be progressively more diffuse. At a bp:CP ratio of about 2 bp to 1 dimer, the band could no longer be clearly identified. Essentially, the same pattern of DNA binding and electrophoretic mobility was observed over a wide range of DNA concentrations (data not shown).

CP–DNA assembly was monitored in solution using changes in the fluorescence of the DNA intercalator ETBR to observe

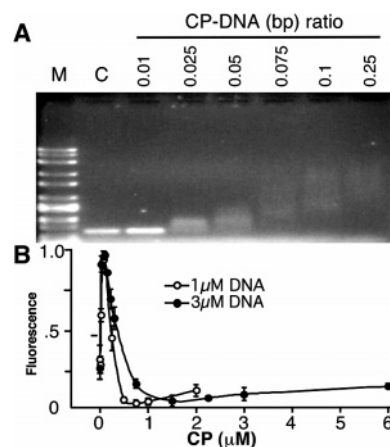


Figure 1. CP binds DNA. (A) CP dimer retards migration of a 500-mer DNA (1 μ M bp) compared to free DNA (control, C). The DNA band is difficult to visualize with a CP:bp molar ratio of ≥ 0.5 . The Cp:bp ratios correspond to 5, 12, 25, 37, 50, and 125 CP dimers/DNA 500-mer. (B) Titration of 1 and 3 μ M bp of an ethidium bromide (ETBR)–DNA complex with CP. At very low CP concentrations (0.01 μ M), there is initial enhancement of fluorescence. Fluorescence decreases at higher CP, suggesting saturation of DNA at 2 bp:CP. ETBR fluorescence was measured at an excitation of 518 nm and an emission of 600 nm.

saturation of the DNA. CP was added to an ETBR–DNA mixture (1:2 molar ratio of ETBR:bp). We saw two transitions: fluorescence increased at low CP and then decreased at higher CP concentration (Figure 1B). The first transition correlated with the appearance of DNA condensates, the second with formation of 17 nm tubes (see below). The solution fluorescence results correlated well with the fluorescence of CP–DNA observed in the gel studies. However, even at saturation, the fluorescence never decreased much below that of the DNA–ETBR complex, which was at least 2 times the intensity of free ETBR, indicating that all or most of the ETBR remained bound to the DNA. In this assay, saturation of the change in ETBR fluorescence appeared at a bp:CP ratio of about 2 bp per CP dimer (250 dimers/DNA 500-mer).

Assembly products, at stoichiometries ranging from 0.5 to 28 DNA bp per dimer (from 1000 to 18 dimers per DNA), were negatively stained with uranyl acetate and examined by transmission electron microscopy (TEM). The products were tubular in shape, of various lengths, but a uniform 17 nm in diameter (Figure 2). The TEM images show that many tubes had a darkly stained lumen, indicating that stain could in some cases penetrate tubes (Figure 2C). Some tubes appeared to have hemispherical caps, which by shape and diameter suggest half of a $T = 1$ capsid.¹² Others had flat ends, suggestive of an opening. Tubes were not branched. ETBR did not affect tube formation.

At higher bp:CP ratios ($\gg 10:1$), very large structures were observed by TEM (Figure 2D). The diameters of these structures were variable, up to ~ 100 nm. As they were progressively more

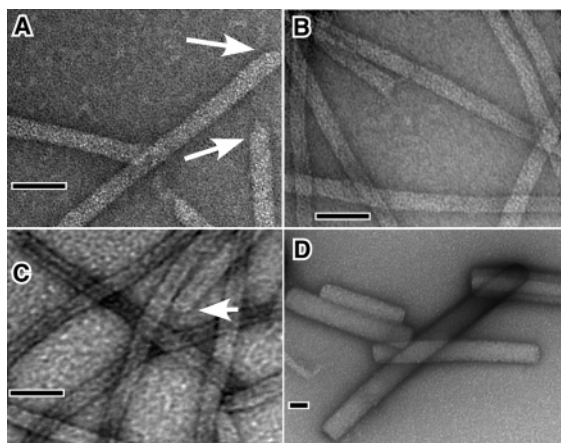


Figure 2. Transmission electron microscopy of in vitro assembled tubular structures. Uranyl acetate stained micrographs of complexes formed at DNA bp:CP dimer ratios of (A) 1:1, (B) 7:1, (C) 14:1, and (D) 28:1. CP tube diameter is a uniform 17 nm, but lengths vary; arrows identify capped ends. DNA condensates (D) have highly variable length and diameter. The scale bars are 50 nm.

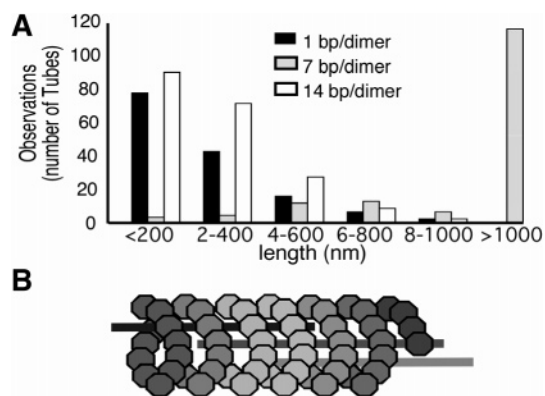


Figure 3. The nature of tubular structures. (A) A histogram shows the wide variation in the length of tubes in micrographs. High and low CP:BP ratios led to a shorter median length. Some tubes formed at 7 bp:CP dimer were longer than 5 μm . Lengths were measured from several micrographs using ImageJ (<http://rsb.info.nih.gov/ij/>).¹⁵ (B) A model of CP–DNA complex, where CP dimers bind nonspecifically to multiple DNA polymers. The ~ 10 nm diameter lumen has ample room for several strands of 2 nm diameter B-form DNA. Though this cartoon indicates helical geometry, we cannot exclude stacks of rings.

common at higher DNA concentrations, we propose that they are DNA condensates.¹¹ Their tubular shape suggested that their growth was nucleated on CP–DNA tubes.

Like the virus they were derived from, the 17 nm CP–DNA tubes were relatively stable. Assembled tubular structures were stable for at least 7 days at 21 $^{\circ}\text{C}$ and 4 $^{\circ}\text{C}$, as judged by TEM. Freezing and thawing led to qualitative disruption of tubes.

There was a consistent steep relationship between length and bp:CP. The lengths of the 17 nm structures ranged from less than 200 nm to over a micron (Figure 3A). Exceptionally long tubes, greater than 5 μm , were formed in reactions where there were 5–10 DNA bp per CP dimer though the median length was 1.35 μm for 7 bp per CP (71 dimer/DNA). At lower (1–5) or higher (10–28)

bp:CP ratios, shorter tubes were seen. The median lengths for 1 and 14 bp:CP (500 and 35 dimer/DNA) were 188 and 237 nm, respectively.

How is the DNA packaged in tubes? Tubes were longer than 170 nm, the maximum length of the 500 bp B-form DNA substrate, suggesting that the DNA was more or less parallel to the tube axis, rather than coiled. Several strands of DNA could be packaged within the ~ 10 nm diameter lumen of the tube to form salt bridges with the CP. It is likely that longer tubes were supported by a scaffold of staggered DNA strands (Figure 3B); lengths were not quantized nor affected by mild sonication (not shown), this also implies that long tubes do not form by association of shorter tubes.

These results led us to propose that tube assembly starts from a nucleation center involving several DNA and CP molecules. The reaction continues for as long as DNA and CP can be recruited to elongate the tube (Figure 3B). Staggering of the DNA facilitates elongation as long as both reactants are present. Shorter tubes resulted when either reactant was limiting. The maximum tube length was observed at 5–10 bp per dimer, a ratio where the negative charge of the DNA roughly matches the +18 positive charge of the two RNA-binding motifs on a dimer. We cannot yet describe details of assembly; a nucleus may elongate bi-directionally or a nucleus may be the capped end of a tube. The 17 nm diameter suggests that caps are $T = 1$ hemispheres;¹² tiling theory describes polymerization of a tube starting at an icosahedral cap.¹³

We have demonstrated an application of virus capsid proteins in generating new materials. These structures are a highly organized scaffold from which more complex two- and three-dimensional networks may be prepared. The tunable length distribution of the CP nanotubes contributes to this utility. Like CCMV capsids,¹⁴ CP nanotubes may also be useful for deposition of materials in their constrained internal cavity.

Acknowledgment. We thank Deborah Willits and Dr. Mark Young for their advice and contributions to this effort. This work was supported by grants from NIH (R01-EB00432-03), NSF (MCB-0111025), and OCAST (HR01-154).

References

- (1) Bancroft, J. B. *Adv. Virus Res.* **1970**, *16*, 99–134.
- (2) Speir, J. A.; Munshi, S.; Wang, G.; Baker, T. S.; Johnson, J. E. *Structure* **1995**, *3*, 63–78.
- (3) Johnson, J. M.; Tang, J.; Nyame, Y.; Willits, D.; Young, M. J.; Zlotnick, A. *Nano Lett.* **2005**, *5*, 765–770.
- (4) Huck, W. T. S.; Tien, J.; Whitesides, G. M. *J. Am. Chem. Soc.* **1998**, *120*, 8267–8268.
- (5) Bowden, N. B.; Weck, M.; Choi, I. S.; Whitesides, G. M. *Acc. Chem. Res.* **2001**, *34*, 231–238.
- (6) Duan, H. W.; Kuang, M.; Wang, J.; Chen, D. Y.; Jiang, M. *J. Phys. Chem. B* **2004**, *108*, 550–555.
- (7) Filankembo, A.; Pileni, M. *J. Phys. Chem. B* **2000**, *104*, 5865–5868.
- (8) Jiang, H.; Lin, W. B. *J. Am. Chem. Soc.* **2003**, *125*, 8084–8085.
- (9) Levin, M. D.; Stang, P. J. *J. Am. Chem. Soc.* **2000**, *122*, 7428–7429.
- (10) Johnson, J. M.; Willits, D.; Young, M. J.; Zlotnick, A. *J. Mol. Biol.* **2004**, *335*, 455–464.
- (11) Conwell, C. C.; Vilfan, I. D.; Hud, N. V. *Proc. Natl. Acad. Sci. U.S.A.* **2003**, *100*, 9296–9301.
- (12) Tang, J.; Johnson, J. M.; Dryden, K.; Young, M. J.; Zlotnick, A.; Johnson, J. E. *J. Struct. Biol.* **2006**, in press.
- (13) Twarock, R. *Bull. Math. Biol.* **2005**, *67*, 973–987.
- (14) Douglas, T.; Young, M. *Nature* **1998**, *393*, 152–155.
- (15) Abramoff, M. D.; Magelhaes, P. J.; Ram, S. J. *Biophotonics Int.* **2004**, *11*, 36–42.

JA056656F